

Supporting Information

Porous Multishelled NiO Hollow Microspheres Encapsulated within Three-Dimensional Graphene as Flexible Free-Standing Electrodes for High-Performance Supercapacitors

Zhifang Zhang,^{#a} Xiaorui Su,^{#a} Yanyan Zhu,^{*a} Zhonghui Chen,^{*b} Zebo Fang,^c Xiaojing Luo^{*a}

Calculation

(1) Determination of the mass ratio of the positive and negative active materials.

The charge of two electrodes has been balanced based on the charge balance principle to obtain an optimum electrochemical performance. The charge is given by the following Formula:

$$\frac{m^+}{m^-} = \frac{C^- \cdot \Delta V^-}{C^+ \cdot \Delta V^+} \quad \text{(Formula S1)}$$

Where C (F g^{-1}) is the specific capacitance, ΔV (V) is the potential window and m (g) is the mass of the active materials. Based on the discharge curve at 1 A g^{-1} , the specific capacitance of the AC electrode is calculated to be 206.3 F g^{-1} . To balance the charge between the positive and negative electrodes, the mass ratio of positive electrode to negative electrode is optimized to be 0.75.

(2) The specific capacitances of ASC devices calculated from GCD curves. Note that when calculating the current density, m refers to the total mass of the positive and negative active materials.

(3) The energy density (E) and power density (P) are calculated according to the following formulas:

$$E = \frac{1}{2} C \cdot (\Delta V)^2 \quad \text{(Formula S2)}$$

$$P = \frac{E}{\Delta t} \quad \text{(Formula S3)}$$

Where E (Wh kg^{-1}) is the energy density, C (F g^{-1}) is the specific capacitance, ΔV is the voltage window, P (W kg^{-1}) refers to the power density and Δt (s) is the discharge time.

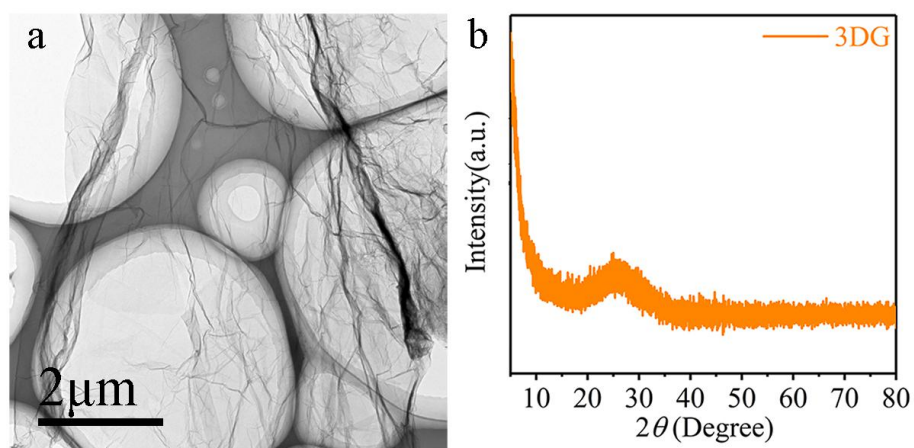


Fig. S1 (a) TEM image and (b) XRD pattern of 3DG.

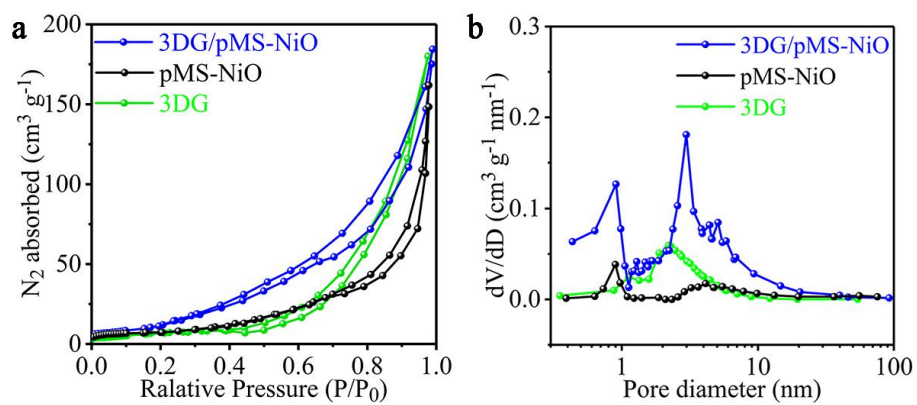


Fig. S2 (a) N_2 adsorption/desorption isotherms and (b) pore size distribution of the 3DG/pMS-NiO, pMS-NiO and 3DG.

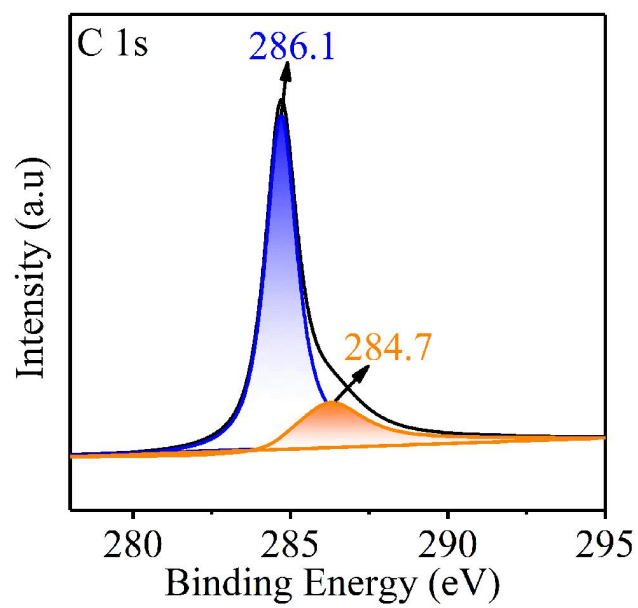


Fig. S3 XPS spectrum of C 1s of the 3DG/pMS-NiO.

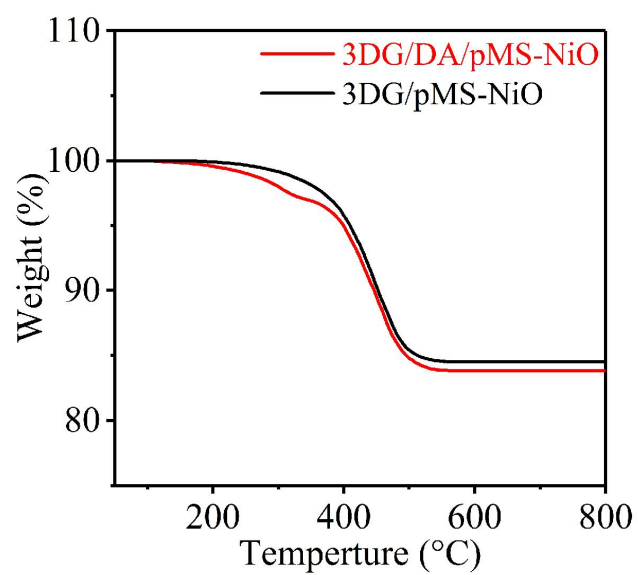


Fig. S4 TGA curves of 3DG/DA/pMS-NiO and 3DG/pMS-NiO in air flow at a rate of 20 °C min⁻¹.

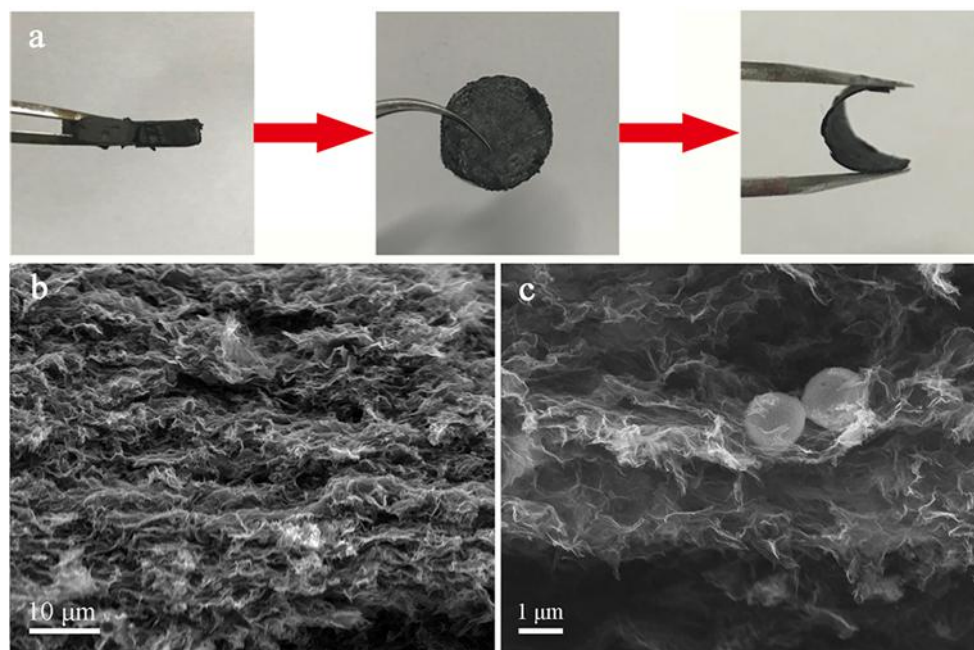


Fig. S5 (a) Preparation of the flexible 3DG/pMS-NiO films, SEM images of (b) the side-view and (c) the interior microstructure of the 3DG/pMS-NiO films at different scale bars.

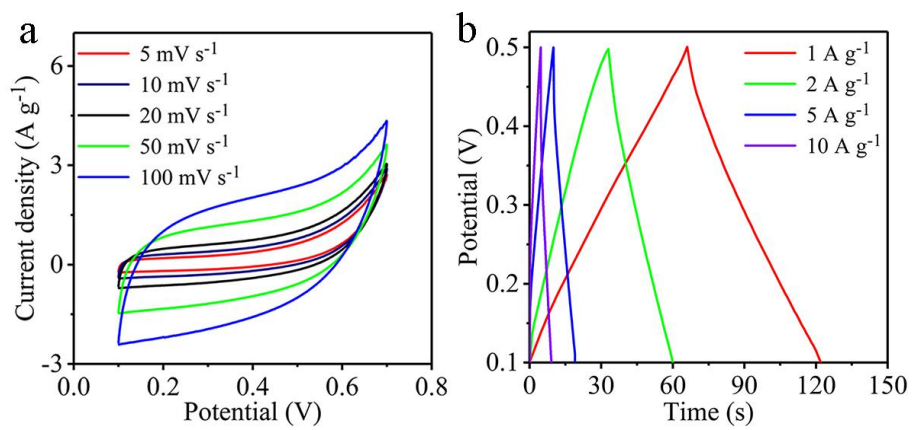


Fig. S6 (a) CV curves of 3DG at different scan rates, (b) GCD curves of 3DG at different current densities.

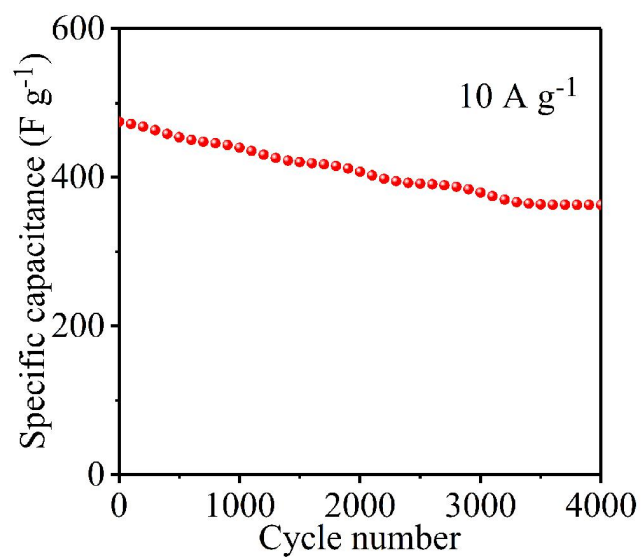


Fig. S7 The specific capacitance of the pMS-NiO electrode after 4000 cycles at 10 A g⁻¹.

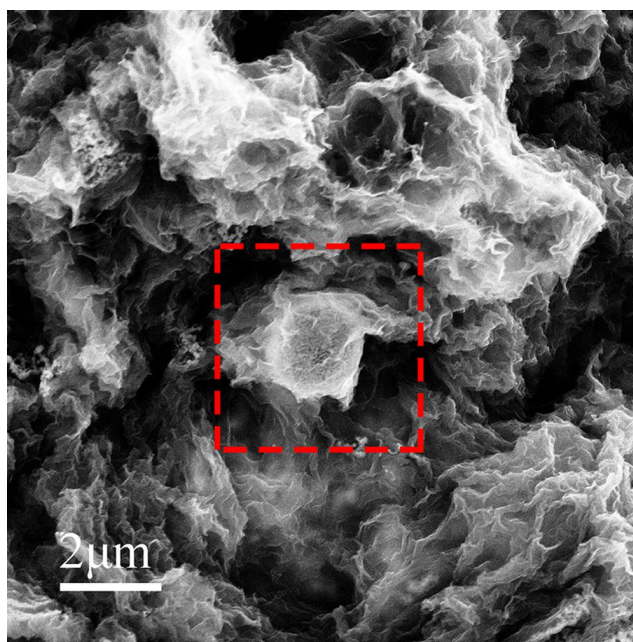


Fig. S8 SEM image of the 3DG/pMS-NiO after cycling tests.

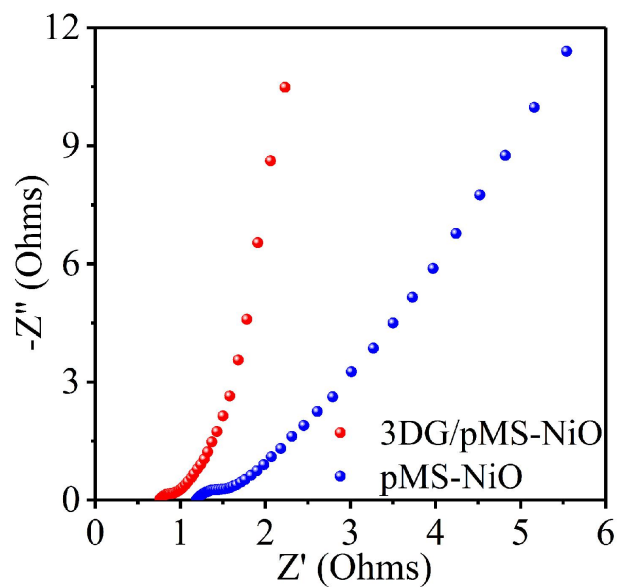


Fig. S9 The Nyquist plots of the 3DG/pMS-NiO and pMS-NiO electrodes.

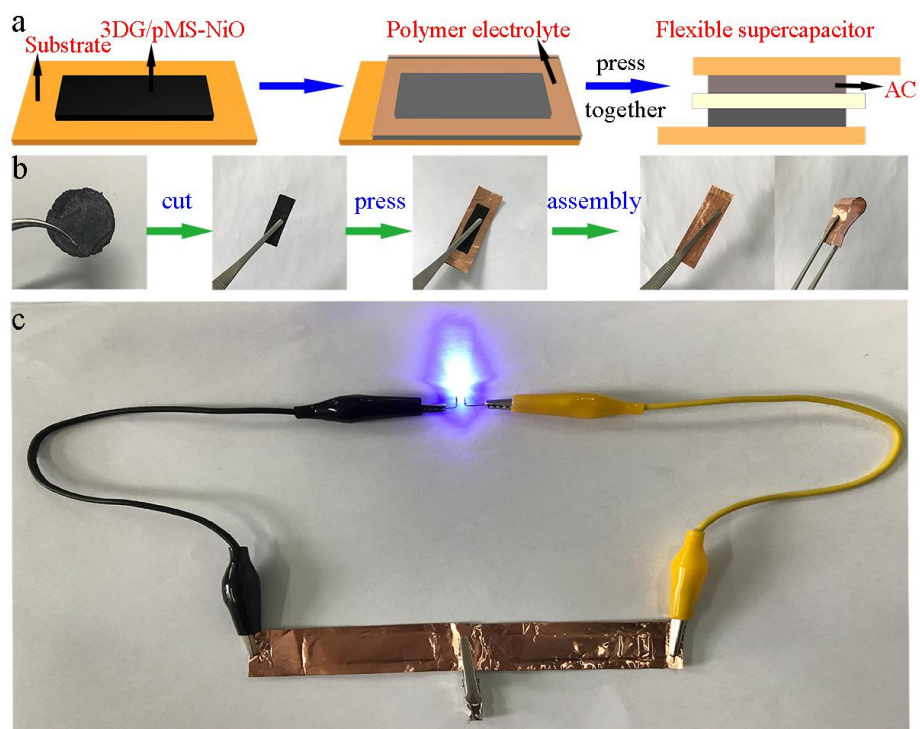


Fig. S10 (a) Schematic diagram and (b) the fabrication process of flexible solid-state supercapacitors. (c) Digital photograph of a LED powered by the two supercapacitors in series.

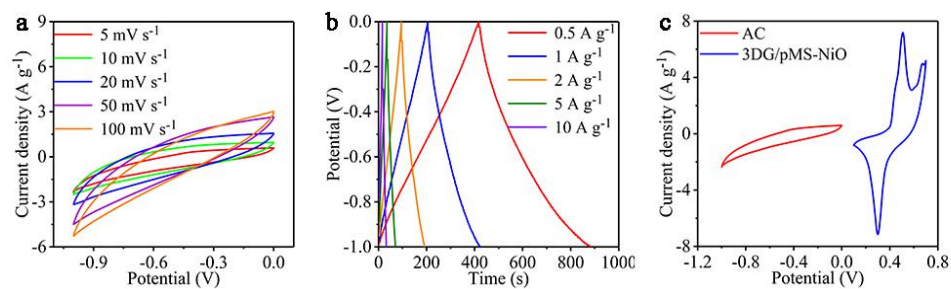


Fig. S11 (a) CV curves at different scan rates and (b) GCD curves at different current densities of the AC electrode. (c) CV curves of the AC and 3DG/pMS-NiO electrodes at 50 mV s⁻¹.

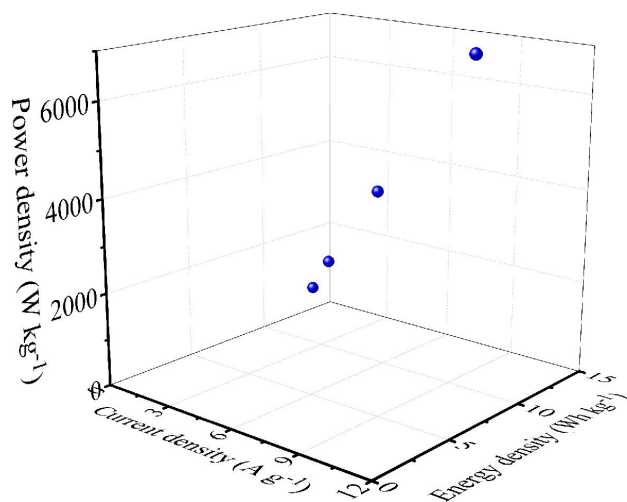


Fig. S12 The energy densities and power densities of the 3DG/pMS-NiO//AC devices at different current densities.

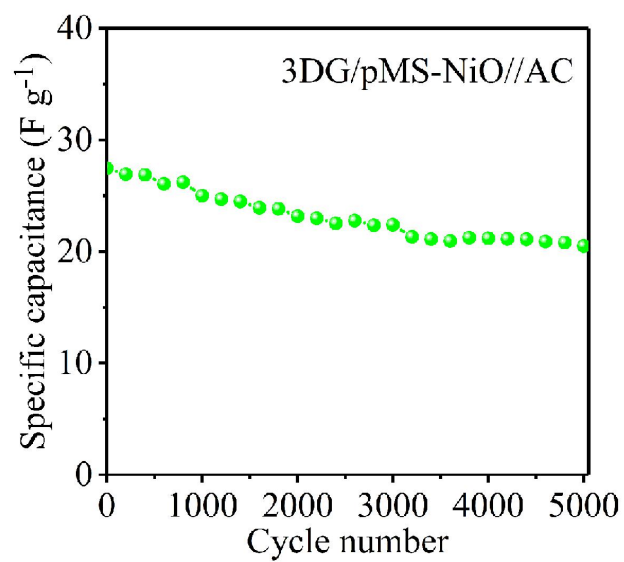


Fig. S13 Cycling performance of the 3DG/pMS-NiO//AC device at 10 A g⁻¹.

Table S1. Comparison of the rate capability of flexible 3DG/pMS-NiO electrodes with other reported NiO-based electrode.

Electrodes	Specific capacitance at low Current density ($F\ g^{-1}$)	Specific capacitance at high current density ($F\ g^{-1}$)	Capacitance retention (%)	Ref.
NiO/UDG/NF	425 at 2 A g^{-1}	300 at 10 A g^{-1}	70.6	S1
NiO HMSs/NFs	809 at 1 A g^{-1}	622 at 10 A g^{-1}	76.9	S2
NiO Hierarchical Nanostructures	456 at 1 A g^{-1}	333 at 10 A g^{-1}	73.1	S3
NiO/Carbon Nanofiber	406 at 2 A g^{-1}	341 at 10 A g^{-1}	83.9	S4
Co ₃ O ₄ -NiO/GF	766 at 1 A g^{-1}	530 at 10 A g^{-1}	69.2	S5
Ni-NiO Foam	924 at 1 A g^{-1}	501 at 8 A g^{-1}	54.2	S6
Ni-NiO Nanoparticles	641 at 1 A g^{-1}	122 at 10 A g^{-1}	19.1	S7
3DG/pMS-NiO	710.4 at 0.5 A g^{-1}/ 692 at 1 A g^{-1} 672.2 at 2 A g^{-1}	657 at 10 A g^{-1}	92.5	This work

Reference

- S1 C. Wu, S. Deng, H. Wang, Y. Sun, J. Liu, H. J. A. A. M. Yan and Interfaces, *ACS Appl. Mater. Inter.*, 2014, **6**, 1106.
- S2 L. Tao, C. Jiang, C. Bei, Y. Wei and J. J. J. o. P. S. Yu, *J. Power Sources.*, 2017, **359**, 371-378.
- S3 J. Min, J. Liu, M. Lei, W. Wang, Y. Lu, L. Yang, Q. Yang, G. Liu and N. J. A. A. M. I. Su, *ACS Appl. Mater. Inter.*, 2016, **8**, 780–791.
- S4 M. Liu, X. Wang, D. Zhu, L. Li, H. Duan, Z. Xu, Z. Wang and L. J. C. E. J. Gan, *Chem. Eng. J.*, 2017, **308**, 240-247.
- S5 R. Waghmode and A. J. J. o. M. S. M. i. E. Torane, *J. Mater. Sci.*, 2016, **27**, 6133-6139.
- S6 M. Mirzaee and C. J. J. o. S. S. E. Dehghanian, *J. Solid State Electrochem.*, 2018, **22**, 3639-3645.
- S7 H. Du, C. Zhou, X. Xie, H. Li, W. Qi, Y. Wu and T. J. I. J. o. H. E. Liu, *Int. J. Hydrog. Energy*, 2017, **42**, 15236-15245.